

Simple model for relating EELS and XAS spectra of metals to changes in cohesive energy

David A. Muller

*Bell Laboratories, Lucent Technologies, Murray Hill, New Jersey 07974
and School of Applied and Engineering Physics, Cornell University, Ithaca, New York 14853*

(Received 25 February 1998)

An explicit connection between the unoccupied single-particle states which are measured with electron energy loss or x-ray-absorption spectroscopy (EELS or XAS) and the occupied states which are involved in bonding is established by applying the force theorem to the tight-binding bond model. The resulting sum rule relates the first moment of the EELS spectrum to the single-particle bond energy. The sum rule connects a local EELS measurement with a local change in cohesion, thus treating the energetics of defects and nonperiodic structures on an equal footing with perfect crystals. As an example, the sum rule is used to estimate the cohesion of a grain boundary in Ni₃Al from experimental EELS spectra. It should also prove useful for qualitative interpretations of EELS spectra in other metal alloys. [S0163-1829(98)01134-5]

I. INTRODUCTION

In many metals and alloys, the segregation of impurities to a grain boundary, can have a dramatic effect on the mechanical properties of the material. The interatomic forces which hold the material together are, at a most fundamental level, determined by the local electronic structure (or using a single-particle description, these are simply the bonds). Understanding the changes in the bonding is a first step towards a quantitative understanding of intergranular fracture. While accurate calculations of electronic structure and cohesion are possible for simple, high symmetry grain boundaries,^{1,2} the structures of more commonly appearing, general grain boundaries are still too complicated to simulate.

However, electronic structure can be measured on an atomic scale using the inelastic scattering of a focused, high-energy electron beam. Electron energy loss spectroscopy (EELS) of the transmitted beam reveals the one-electron conduction-band density of states (DOS) partitioned by element, site, and angular momentum.^{3,4} Similar information can also be obtained with x-ray-absorption spectroscopy (XAS),⁵ although the lateral spatial resolution is currently a factor of 200 worse.^{6,7} With recent improvements in the stability and detection efficiency of modified scanning transmission electron microscopes (STEM), it has become possible to apply the electron spectroscopy to the study of grain boundaries and buried interfaces using atomic-sized probes.⁸⁻¹⁰

For instance, EELS measurements have shown that boron has a profound effect on the electronic structure of grain boundaries in Ni₃Al,¹¹⁻¹³ an effect that could be correlated with the change in fracture mode and environmental embrittlement of the boundaries when bulk ingots of Ni₃Al are doped with a 200–1000 ppm of boron.¹⁴ Spatially resolved EELS is particularly well suited to the study of both the composition and electronic structure changes that occur at grain boundaries. More recently, changes in the electronic structure of copper at bismuth-doped copper grain boundaries have been reported.¹⁵ EELS can also provide direct checks of the calculated electronic structures of phosphorus, carbon and boron at iron grain boundaries.^{1,2}

The one drawback to the EELS measurements is that

EELS (and the same is true of XAS) measures only the empty, single-particle states. However, only occupied states are involved in the bonding. The purpose of this paper is to provide a quantitative relationship between the unoccupied states measured with EELS and the bond energy contribution to the changes in cohesive energy that might occur at a grain boundary, defect or different alloy compositions.

The resulting “sum rule” is also useful for describing bonding trends in transition metals and their alloys, greatly simplifying the interpretation of EELS spectra. In general, a tall, narrow peak at the onset of a transition-metal *L* edge (EELS or XAS) implies weaker bonding for that atom than if the *L* edge peak was short and broad. This rule of thumb explains the trends in the bonding at the grain boundaries in the Ni₃Al:B (Ref. 12) and Cu:Bi (Ref. 15) systems.

There are three key approximations made in deriving the sum rule: firstly, it is assumed that the EELS excitation spectrum should resemble the true quasiparticle density of states, which implies that the core hole and excitonic effects are sufficiently well screened that they cannot be observed in the experiment. This is generally found to be the case for transition-metal spectra³ and the Ni-Al system in particular.¹⁶

Secondly, the changes in the electron density around the atoms to be compared are assumed to be small. When this holds, Anderson’s force theorem¹⁷ states that the changes in the total energy are given, to first order, by changes in the single-particle eigenvalues and the remaining many-body effects enter only as higher-order corrections. These corrections are important in strongly correlated systems. In ionic systems, the bond energies are smaller than the electrostatic energies and again, the single-particle picture is not complete. This will limit the application of the sum rule to covalent and metallic systems. Further, the force theorem, is expected to be more accurate for internal defects and grain boundaries than for free surfaces and absorbed monolayers where the density changes are more dramatic.

Thirdly, the system is assumed to be a good metal with a well defined Fermi energy. This obviously restricts the range of suitable systems, but is important for relating energy shifts in the core levels to shifts in the valence band. It also has the benefit of ensuring that the screening is sufficiently effective

to minimize charge transfers, which would otherwise complicate the calculation of the energy differences.

The consequence of all three approximations can be experimentally tested and such tests will be described for the bulk Ni-Al alloys in the final section of this paper. First, brief outlines of electron energy loss spectroscopy, the force theorem, and the tight-binding-bond model will be given. Section IV contains the actual derivation of the tight-binding/EEL sum rule. Finally, quantitative comparisons of the cohesive energies calculated using the tight-binding/EELS sum rule are described in Sec. V.

II. EELS AND ELECTRONIC STRUCTURE

EELS (and XAS) probes excitations of core electrons which occur at unique energy losses for each element. For example, the Ni L edges ($L_2:2p_{1/2} \rightarrow d_{3/2}$ and $L_3:2p_{3/2} \rightarrow d_{3/2}, d_{5/2}$) at 870 and 853 eV energy loss, respectively, select excitations from the Ni $2p$ orbitals to states above the Fermi level. From Fermi's golden rule and dipole selection rules, the observed intensity is proportional to a local density of states (LDOS) with s -like or d -like symmetry in the conduction band.^{18,19,5} However, the transitions to s -like final states are so much weaker than to d -like final states that only the latter need be considered (this is true for all the $3d$ transition metals). It should be noted that for the Al L edge, transitions to s -like and d -like final states occur with roughly equal probability.¹⁶ The overlap of the final state with the very localized $2p$ initial state, defines the measured LDOS to be proportional to a muffin-tin projected DOS (and differing from it only by a matrix element that is slowly varying with energy⁵). The EELS core-edge oscillator strength is also proportional to a linear combination of atomiclike orbitals (LCAO) basis over the energy range for which the LCAO basis is complete.¹⁶ The LCAO description is more intuitive for dealing with basis-dependent quantities such as charge transfers, and will be used in this paper unless otherwise noted. For single electron excitations, the near-edge fine structure in EELS thus reflects the unoccupied local density of states of the solid (in this case the Ni d DOS). As every element has a unique set of core-level binding energies, the core-level excitations partition the local density of states by element in addition to site and angular momentum.

III. THE FORCE THEOREM

The ground-state total energy of a system, considering only the valence electrons, can easily be a few hundred eV per atom (this is the energy required to assemble the system from its constituent electrons and ion cores). However the energy changes per atom expected at grain boundaries and defects are on the order of an eV per atom or less. It would then be a formidable task if it were necessary to approximate the total energy of a system in order to determine the energies of such structures. Fortunately there is a remarkably simple theorem which makes the calculation of energy differences from a known structure (even a free atom) very tractable. This is the "force theorem" of Pettifor^{20,21} and Mackintosh and Anderson.¹⁷ Discussion of its derivation and implications can be found in Refs. 22,23. It states that given a self-consistent solution to the Kohn-Sham equations, the

first-order change in total energy, δE is given by

$$\delta E = \delta \left(\sum_i n_i \epsilon_i \right) + \delta E_{es}. \quad (1)$$

The first term is the change in the occupied one-electron states of energy ϵ_i and occupancy n_i , calculated using the displaced (by the perturbation) but otherwise frozen one-electron potential. δE_{es} is the change in the classical electrostatic energy. If the cell defining the perturbed atom were neutral and spherically symmetric then δE_{es} would be zero. Otherwise it would be the change in the Madelung energy. When choosing to work with a charge neutral system, a first-order *change* in the total energy is given simply by the change in the Kohn-Sham single-particle eigenvalues.

The total energy itself is not given by the eigenvalue sum alone but the energy difference is. The key result of the force theorem is that the double counting terms in the Coulomb energy have been canceled out. Although these exchange and correlation energies make an important contribution to the total energy of the solid, they do not contribute to a first-order change in the total energy. This follows from the self-consistent Kohn-Sham equations being at an variational minimum in the charge density ρ . Hence $\delta E / \delta \rho$ is zero and there is no first-order contribution from $\delta \rho$.

The force theorem appears to explain the success of tight binding and molecular orbital theory in predicting structures and heats of formation from eigenvalue sums, when the sum themselves are not good descriptions of the total energy.

In working with systems that maintain an approximate local charge neutrality (i.e., $\delta E_{es} = 0$, as discussed above), we need only retain the first term of the force theorem [Eq. (1)]:

$$\delta E \approx \sum_i n_i (\delta \epsilon_i) + \sum_i (\delta n_i) \epsilon_i. \quad (2)$$

The first term is recognized as the bond energy, and the second term is the promotion energy.²⁴⁻²⁶ These energies have simple chemical interpretations when the reference system is chosen to be a free atom, with orbitals at energies $\{\epsilon_a\}$. (As we will always be comparing differences in bond and promotion energies, the choice of reference is arbitrary.) With respect to the free atom, the bond energy can be rewritten as

$$U_{\text{bond}} = \sum_a \int_{-\infty}^{E_F} (E - \epsilon_a) n_a(E) dE, \quad (3)$$

where $n_a(E)$ is the a projected LDOS and E_F is the Fermi energy (for simplicity only metals at $T=0$ K are considered—a Fermi function must be introduced at finite temperatures). This describes the covalent bonding and broadening of discrete state into bands that occurs when a solid is formed from free atoms. States lower in energy than that of the free atom are termed bonding states (as they lower the bond energy). States at higher energies than the free atom are antibonding—Eq. (3) changes sign at $E = \epsilon_a$. In many tight-binding calculations, overlap with the core states on neighboring sites is neglected which results in a bond energy that is always attractive.^{27,28} If the nonorthogonality between the model orbitals on different sites is considered, this cre-

ates an asymmetry between bonding and antibonding states, allowing for strong repulsions at short interatomic spacings. This feature is not present in the densities of states calculated from orthogonal tight-binding schemes where the repulsions are often modeled with pair potentials instead.^{25,28} This problem is removed by dealing with the experimental density of states (which should have the appropriate asymmetry), rather than a model density of states.

The promotion energy U_{prom} takes into account the change in occupancy of the orbitals on forming the solid from the reference system.

$$U_{\text{prom}} = \sum_i \delta n_i \epsilon_i. \quad (4)$$

If the system is kept charge neutral then these will be the only contributions to the force-theorem calculated binding energy. In metals where the screening length is typically shorter than the interatomic separation, it is a fair approximation to assume each site remains charge neutral.²⁹

The simplest modeling of this screening is to impose a local charge neutrality on the system. This can be done by either rigidly shifting all the diagonal Hamiltonian matrix elements on a given atom by the same amount^{29,25} or by adjusting the individual atomic orbital³⁰ (in which case the promotion energy is zero). In both cases, the calculation must be iterated to self-consistency. From the force theorem we know that a self-consistent redistribution of charge does not contribute to the force on the atom so the bond energy is calculated with respect to the self-consistently determined on-site energies.

The strongest motivation for the assumption of charge neutrality in the present work is experimental. First, the number of Ni d holes measured by EELS in Ni, Ni₃Al, and NiAl do not vary by more than 2%.¹⁶ This is confirmed by linear-augmented plane-wave (LAPW) calculations of the EELS oscillator strengths. When integrated over either the valence band or the unoccupied states (0–14 eV above the Fermi energy), these also did not change by more than 2% for the d states in Ni, Ni₃Al and NiAl.¹⁶ If the EELS spectra are interpreted in terms of a LCAO basis, this implies the LCAO charge transfers are less than 0.1 e /atom. (A rough rule-of-thumb as to when charge transfers are likely to cause this approximation to fail is discussed in Sec. V).

Second, the self-consistent shift of the orbitals to ensure a local charge neutrality results in a small, but measurable core-level shift.³¹ In the Ni-Al system, this core-level shift required to preserve local charge neutrality is within experimental error of the experimentally measured core-level shift.³² These experimental measurements seem to favor the picture of orbital charge neutrality (keeping the number of electrons in each orbital fixed) over that of site neutrality (which involves a small s - d charge transfer) but this may be an artifact of the Wolfsberg-Helmholtz approximation used in the extended Hückel calculations.³² Orbital neutrality may be too restrictive for modeling semiconductors where s - p promotions can occur.

A key result of the force theorem (Sec. III) is that changes in bond energy (and hence also the cohesive energy) are directly related to the local density of states through Eq. (3). Consequently, understanding the shape of the LDOS can also

help us to understand the cohesion and stability of a given structure. In Sec. IV this idea is used to related the measured EELS spectra to grain-boundary energies.

IV. THE RELATIONSHIP BETWEEN EELS AND THE BOND ENERGY

In a single-particle picture, EELS probes the unoccupied electronic states in a material [this is found to be a good approximation for Ni, Ni₃Al, and NiAl (Ref. 16)]. However the ground-state properties of a material depend only on the occupied states. The challenge is then to infer the properties of the filled states from the empty ones. Here that connection is made for metals that can be modeled with an atomic basis set. The advantage of a tight-binding basis (both orthogonal and nonorthogonal) is that the moments are well defined. For a more general basis, often only the changes in a given moment are defined. A derivation of desired sum rule for measuring energy differences from EELS is more tedious for a general basis, but the result is the same.³³

In either case, the dominant contribution to the cohesive energy is the bond energy term of Eq. (3), U_{bond} . In general, the contribution from every valence orbital is needed. For clarity, only the d states will be considered in this section—the general case can be recovered simply by summing over all the valence states. The d states are of particular interest as in the Ni-rich Ni-Al alloys, the Ni d DOS is the dominant contribution (see Ref. 16). The same is likely to be the case in most transition-metal-rich systems.

The starting point for the connection between the EELS measurements and the bond energy is to note that the first moment of the density of states (both filled and empty) is defined as

$$\mu^{(1)} = \int_{-\infty}^{\infty} (E - \epsilon_d)^{(1)} n_d(E) dE. \quad (5)$$

In a tight-binding basis $\mu^{(1)} = 0$ (A proof of this follows trivially from Cyrot-Lackmann's moments theorem^{34,23} as $\mu_i^{(1)} = \langle i | H - \epsilon_i | i \rangle$ and $\langle i | H = \langle i | \epsilon_i$). The treatment for an arbitrary form of $\mu^{(1)}$ is given in Ref. 33.

In the experimental system, the only physically measurable reference energy is the Fermi energy, E_f . Choosing this as the origin, i.e., $E_f = 0$, and trivially separating the integral over the occupied and unoccupied states, Eq. (5) becomes (as $\mu^{(1)} = 0$)

$$0 = \int_{-\infty}^0 (E - \epsilon_d) n_d(E) dE + \int_0^{\infty} (E - \epsilon_d) n_d(E) dE. \quad (6)$$

Notice that the first term on the right-hand side is simply the bond energy. The second term depends only on the unoccupied DOS, which is measurable by EELS.

Now we define the first moment of the EELS spectrum as

$$m^{(1)} = \int_0^{\infty} E n_d(E) dE. \quad (7)$$

The zeroth moment is the number of unoccupied states, i.e., the number of d holes,

TABLE I. EHT calculated $\Delta\epsilon_d$ and the measured L_3 -edge core-level shifts, ΔE_{L_3} , from Ref. 32. For the EELS sum rule to apply $\Delta\epsilon_d \approx \Delta E_{L_3}$. There is a 0.1 eV systematic error in the EHT parameters. Differences are measured with respect to bulk Ni (in eV).

	$(E_F - \epsilon_d)$	$\Delta(E_F - \epsilon_d)$	E_{L_3}
Ni	1.45		
Ni ₃ Al	1.55	0.10 ± 0.1	0.08 ± 0.05
NiAl	1.97	0.52 ± 0.1	0.60 ± 0.1

$$H_d = \int_0^\infty n_d(E) dE. \quad (8)$$

Substituting these two definitions in Eq. (6), we obtain a first moment sum rule relating the EELS spectrum to the bond energy:

$$-U_{\text{bond}} = m^{(1)} - \epsilon_d H_d. \quad (9)$$

Now consider two atoms i, j of the same species that are in slightly different environments. For such conditions the force theorem gives $\Delta E_{\text{cohesive}} \approx \Delta U_{\text{bond}}$. The very effective screening in the metal is approximated by assuming a local charge neutrality so $N_i = N_j$ and $H_i = H_j$. Then

$$\Delta U_{\text{bond}} = U_{\text{bond}_i} - U_{\text{bond}_j} = H_d \Delta\epsilon_d - \Delta m_d^{(1)}, \quad (10)$$

where

$$\Delta m_d^{(1)} = m_{i,d}^{(1)} - m_{j,d}^{(1)}, \quad (11)$$

$$\Delta\epsilon_d = \epsilon_{i,d} - \epsilon_{j,d}.$$

As a practical matter, a general density of states may be unbounded, and it is better to calculate $\Delta m_d^{(1)}$ as

$$\Delta m_d^{(1)} = \int_0^\infty [n_{i,d}(E) - n_{j,d}(E)] dE \quad (12)$$

as both $n_{i,d}$ and $n_{j,d}$ tend to the same free-atom-like value, at large energies (a high-energy electron is only weakly affected by the valence states).

The difference in bond energies between two sites can be determined from the first moment of the EELS spectra from those sites provided $\Delta\epsilon_d$ and H_d are known. The number of holes can be determined from a band-structure calculation for the reference site. The valence band shifts often can be determined from the core-level shifts, and this is indeed the case for the Ni-Al compounds.^{32,33} Table I shows the extended Hückel (EHT) calculated $\Delta\epsilon_d$ for the ordered Ni-Al alloys and the measured core-level shifts.^{32,33} In general, the core-level shift will only track the valence-band shift, if the differences in ‘‘final-state’’ effects (due to the creation of a core hole) are small. This seems to be a good approximation for transition metals,³¹ although it is known to fail at some noble-metal surfaces^{35,36} where screening is less effective. For this work, errors of 0.1 eV or less are tolerable as this is comparable to the precision of the experimental measurements.

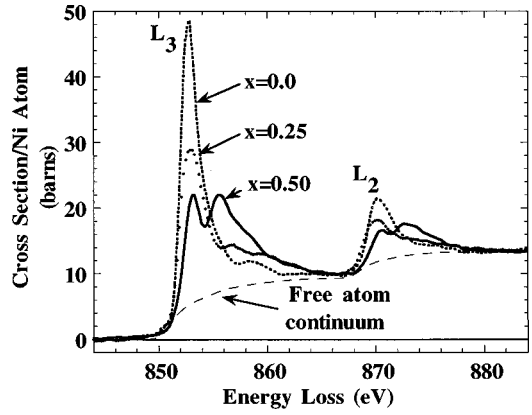


FIG. 1. Ni L_3 edge recorded at the large angle boundary in undoped Ni₃Al. Ni L_3 edge recorded at the large angle boundary in undoped Ni₃Al and compared to a spectrum taken far from the boundary (bulk).

Returning to the first-moment ‘‘sum rule,’’ and assuming $\Delta E_{L_3} \approx \Delta\epsilon_d$, the change in bond energy can be now rewritten *solely* in terms of quantities measurable by EELS:

$$\Delta U_{\text{bond}} \approx \Delta E_{L_3} H_d - \Delta m_d^{(1)}. \quad (13)$$

If there is no core-level shift then Eq. (13) allows us to determine qualitative trends in the bond energy from the shape of the EELS spectrum:

If the edge shape changes from sharply peaked at the onset to flatter and broader, then the bond strength has also increased (as the first moment of that EELS spectrum has increased). These trends are easily seen in Fig. 1 where the Ni $L_{2,3}$ edge for bulk Ni₃Al is compared with the Ni edge from a grain boundary in undoped Ni₃Al. The reduced first moment of the boundary spectrum (it has a larger peak at the edge onset than the bulk) implies a loss of bonding at the grain boundary.

V. QUANTITATIVE TESTS OF THE TIGHT-BINDING/EELS SUM RULE

The tight-binding/EELS sum rule of Eq. (13) will probably prove most useful for offering a qualitative explanation of bonding changes. However, it can also provide quantitative information on the bonding in metals, provided sufficiently complete and noise-free spectra can be recorded. Quantitative analysis is restricted to metallic systems as the core-level shift can only be related to valence band shift if there is a well-defined Fermi energy.³² (Qualitative discussion is still possible for small-gap semiconductors, provided the charge transfers remain small.) If small charge transfers do occur, the method will be in error by the neglected difference in Madelung energies. As a rough rule-of-thumb, the sum rule should not be applied if the Pauling ionicity exceeds 10% (Ref. 37). (The Fe:B, Fe:P, Cu:Bi, and Ni:Al systems all satisfy this rule very comfortably.)

In this section, experimentally measured EELS spectra from bulk Ni-Al compounds are used to test the accuracy of the tight-binding/EELS sum rule in estimating the heats of formations of the compounds.

The heat of formation of a compound from its bulk con-

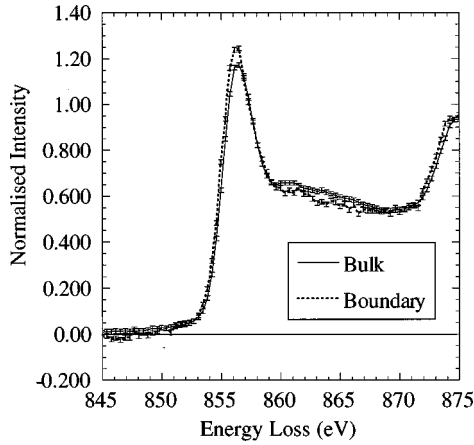


FIG. 2. Measured Ni $L_{2,3}$ edge (after deconvolution and background subtraction) for the $\text{Ni}_{(1-x)}\text{Al}_x$ system showing the decrease in height and broadening of the sharp peak (“white line”) at the onset of the L_2 and L_3 edges with increasing Al concentration. The spectra are scaled to the atomic Ni cross section (see text). The statistical errors in the measured spectra are indicated by the plotted line thickness. There is also a 2–5 % systematic error in the background subtraction.

stituents is defined in the usual way, in this case

$$\Delta H(\text{Ni}_{(1-x)}\text{Al}_x) = U_{\text{Coh}}(\text{Ni}_{(1-x)}\text{Al}_x) - (1-x)U_{\text{Coh}}(\text{Ni}) - xU_{\text{Coh}}(\text{Al}). \quad (14)$$

Applying the force theorem, this becomes

$$\Delta H(\text{Ni}_{(1-x)}\text{Al}_x) \approx U_{\text{bond}}(\text{Ni}_{(1-x)}\text{Al}_x) - (1-x)U_{\text{bond}}(\text{Ni}) - xU_{\text{bond}}(\text{Al}). \quad (15)$$

In applying the sum rule of Eq. (13) to obtain the bond energies, it will be assumed that the Ni d states are the dominant contribution to the Ni DOS (this is a good approximation as shown in Ref. 16). In Al, the s and p states are also important. In principle, the Al K and L edges could provide this information.

The experimental spectra are recorded on a 100 kV VG-HB501 STEM equipped with a McMullan style³⁸ parallel energy-loss spectrometer. The experimental method and precautions are described in Refs. 12,16,33. The Ni L edges are all scaled so that they match the atomic cross section in a window between 30 and 40 eV above the L_3 edge. This is sufficiently far above the L_2 edge that the EELS near-edge fine structure has been damped out. The remaining extended fine structure is slowly varying and oscillatory about the atomic cross section (see, Müller and Wilkins⁵). The scaling normalizes the measured intensity to a cross section per Ni atom. Consequently, concentration and thickness dependences are removed and comparisons of the relative cross section per Ni atom can be made as shown in Fig. 2. (The purpose of the analysis is to determine energy changes per atom, not composition, for which standard techniques already exist⁴). Of course, for this to work, multiple-scattering effects (in particular additional valence losses) must first be removed and this is done using a Fourier-ratio deconvolution.^{39,40}

TABLE II. Calculated changes in the first moment of the unoccupied Al DOS compared to the first moment of the measured Al $L_{2,3}$ edge (which reflects both the s and d states in roughly equal weightings). The EELS spectra are normalized to the same areas as the Al DOS so the changes are in eV.

	Al s	Al p	Al d	Al $s+d$	Al $L_{2,3}$
Ni_3Al	0.40	-0.46	0.40	0.80	0.88 ± 0.1
NiAl	0.32	+0.40	0.18	0.50	0.52 ± 0.1

If the spectra are further scaled to that of the LAPW calculated DOS for Ni_3Al (Ref. 16) (which is in good agreement with the EELS spectrum of bulk Ni_3Al) then the energy differences can be determined in eV/Ni atom. The area from the edge onset to 14 eV above the L_3 edge is $H_d = 2 \pm 0.05e^-$ for Ni, Ni_3Al , NiAl , and Ni_3Si (these are the calculated oscillator strengths for the respective solids, not free atoms).¹⁶ Thus prepared, the Ni L_3 edges can now be used to estimate changes in the bond energy per Ni atom. Before doing so, a similar treatment is attempted for the Al atoms.

Accurate measurements of the Al $L_{2,3}$ are more difficult as it is 6 eV above the onset of the Ni $M_{2,3}$ edge. The treatment and processing of the Al $L_{2,3}$ edges can be found in Refs. 16,33. The signal at the Al K edge in Ni_3Al and NiAl was too weak to observe the small changes in the EELS fine structure. Instead, the calculated LAPW DOS (Ref. 16) (for Al, NiAl , Ni_3Al) are used, after being processed and treated like experimental spectra. Table II shows the first moments of the unoccupied Al partial DOS calculated using Eq. (7). Also shown are the first moments of the experimentally measured Al $L_{2,3}$ edges from Ref. 16. The Al L edge contains roughly equal contributions from both s - and d -like states, and as shown in Table II, the first moment of the measured L edge is in very good agreement with the sum of the Al $s+d$ moments.

We are now in a position to test the accuracy of Eq. (13) when applied to an experimental spectrum. Using the core-level shifts from Table I and $H_d = 2 \pm 0.05e^-$, the Ni d state bond energies for Ni_3Al and NiAl (with respect to bulk Ni) are shown in Table III. In Ni_3Al where the d states dominate, ΔU_{bond} is in good agreement with the experimentally measured heat of formation. In NiAl where the Al states have a large influence on the shape of the total DOS, the Ni d state contribution to ΔU_{bond} cannot be compared directly with the heat of formation.

TABLE III. Bond energies changes, $\Delta U_{\text{bond}}(\text{Ni}d)$, calculated from the experimentally measured Ni L_3 edges using the the EELS sum rule [Eq. (13)]. $\Delta U_{\text{bond}}(\text{Al})$ are obtained from treating the calculated Al s,p,d states of Ref. 16 as experimental spectra. The measured heat of formation, ΔH , is from Hultgren *et al.* (Ref. 41). Differences are measured with respect to bulk Ni and Al. The aluminum contribution is small for Ni_3Al but cannot be ignored for NiAl .

	$\Delta U_{\text{bond}}(\text{Ni}d)$ (eV)	$\Delta U_{\text{bond}}(\text{Al})$ (eV)	Calculated ΔH (eV)	Measured ΔH (eV)
Ni_3Al	-0.30 ± 0.1	-0.54 ± 0.1	-0.36 ± 0.1	-0.38 ± 0.05
NiAl	$+0.03 \pm 0.1$	-1.10 ± 0.1	-0.44 ± 0.1	-0.61 ± 0.05

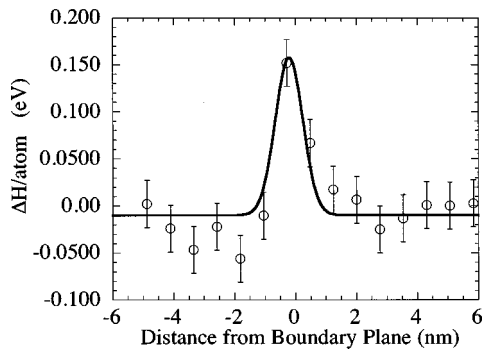


FIG. 3. Spatial variation of the bond energy/per Ni atom across the boundary in undoped Ni_3Al . The bond energy is determined from the measured Ni L_3 edge using the EELS sum rule of Eq. (13).

Figure 3 shows the spatial variation in bond energy/Ni atom across the large-angle grain boundary of Fig. 1 using the normalized EELS spectra and Eq. (13). The energies are quite comparable to the bond energies determined by the real-space models discussed in Refs. 12,32. It is important to realize that the energies are expressed as a bond energy per Ni atom. The Ni concentration profile must also be known to convert the results to a boundary energy per unit area. This can be determined from either the annular dark image or energy dispersive x-ray spectroscopy. If an Al EELS edge is also recorded then the EELS signal could be used. In practice however, the Al K edge is too weak and the background too uncertain on the Al L edge in the Ni-Al alloys for accurate concentration measurements to be made with EELS.

VI. SUMMARY

An explicit connection between the unoccupied single-particle states which are measured with EELS or XAS and the occupied states which are involved in bonding is established by applying the force theorem to the tight-binding bond model. The resulting tight-binding sum rule relates

changes in the first moment of the EELS spectrum to changes in the single-particle bond energy. For the special case where no core-level shift or charge transfers occur, if an EELS edge changes from sharply peaked at the edge onset to a broader shape, then the bond energy has also increased. Explicit knowledge of atomic coordinates is not needed (other than knowing local concentrations) and the changes in cohesion can be modeled solely with information contained in the EELS spectra.

As an example, the sum rule was used to estimate the cohesion of a grain boundary in Ni_3Al . It should also prove useful for qualitative interpretations of EELS spectra in other metal alloys. The model should not be used for insulators, ionic materials, and highly correlated systems where screening is less effective, core hole effects are larger, and single particle descriptions are less appropriate than in simple metals.

A final point to be noted is that the first moment of the EELS spectrum weights contributions from higher energies more heavily than those near the edge onset. This makes the bond energies determined from Eq. (13) very sensitive to errors in background subtraction and noise in general. Quantitative results can only be obtained from very high-quality spectra, and then only with an accuracy of 0.1 eV/atom at best. A more useful role for the first-moment sum rule is in a qualitative discussion of bonding trends. It serves as an existence proof that the properties of occupied states can be determined from knowledge of the unoccupied states.

ACKNOWLEDGMENTS

This research was funded by DOE Grant No. DE-FG02-87ER45322. The Cornell STEM was acquired through the NSF (DMR-8314255) and is operated by the Cornell Materials Science Center (DMR-9121654). Useful discussions with John Silcox are acknowledged. The Ni_3Al boundary was grown by C.T. Liu of ORNL and prepared for microscopy by Shanthi Subramanian.

- ¹R. Wu, A. J. Freeman, and G. B. Olson, *Science* **265**, 376 (1994).
- ²R. Wu, A. J. Freeman, and G. B. Olson, *Phys. Rev. B* **53**, 7504 (1996).
- ³R. D. Leapman, L. A. Grunes, and P. J. Fejes, *Phys. Rev. B* **26**, 614 (1982).
- ⁴R. F. Egerton, *Electron Energy Loss Spectroscopy in the Electron Microscope*, 2nd ed. (Plenum, New York, 1996).
- ⁵J. E. Müller and J. Wilkins, *Phys. Rev. B* **29**, 4331 (1984).
- ⁶H. Ade *et al.*, *Science* **258**, 972 (1992).
- ⁷H. Ade, in *Microscopy and Microanalysis*, edited by G. W. Bailey *et al.* (San Francisco Press, San Francisco, 1996).
- ⁸P. E. Batson, *Nature (London)* **366**, 728 (1993).
- ⁹N. D. Browning, M. M. Chisholm, and S. J. Pennycook, *Nature (London)* **366**, 143 (1993).
- ¹⁰D. A. Muller, Y. Tzou, R. Raj, and J. Silcox, *Nature (London)* **366**, 725 (1993).
- ¹¹D. A. Muller, Y. Tzou, R. Raj, and J. Silcox, in *Defect Interface Interactions*, edited by E. P. Kvam *et al.*, MRS Symposia Proceedings No. 319 (Materials Research Society, Pittsburgh, 1994), p. 299.
- ¹²D. A. Muller, P. E. Batson, S. Subramanian, S. L. Sass, and J. Silcox, *Phys. Rev. Lett.* **75**, 4744 (1995).
- ¹³D. A. Muller, P. E. Batson, S. Subramanian, S. L. Sass, and J. Silcox, *Acta Metall. Mater.* **44**, 1637 (1996).
- ¹⁴C. T. Liu, C. L. White, and J. A. Horton, *Acta Metall.* **33**, 213 (1985).
- ¹⁵J. Bruley, V. Keats, and D. B. Williams, *J. Appl. Phys.* **29**, 1730 (1996).
- ¹⁶D. A. Muller, D. J. Singh, and J. Silcox, *Phys. Rev. B* **57**, 8181 (1998).
- ¹⁷A. R. Mackintosh and O. K. Anderson, in *Electrons at the Fermi Surface*, edited by M. Springford (Cambridge University Press, London, 1980), Chap. 5.3.
- ¹⁸M. Brown, R. E. Peierls, and E. A. Stern, *Phys. Rev. B* **15**, 738 (1977).
- ¹⁹L. F. Mattheiss and R. E. Dietz, *Phys. Rev. B* **22**, 1663 (1980).

- ²⁰D. G. Pettifor, *Commun. Phys.* **1**, 141 (1976).
- ²¹D. G. Pettifor, *J. Chem. Phys.* **69**, 2930 (1978).
- ²²V. Heine, in *Solid State Physics*, edited by H. Ehrenreich and F. Seitz (Academic, New York, 1980), Vol. 35, p. 1.
- ²³A. P. Sutton and R. W. Balluffi, *Interfaces in Crystalline Materials* (Clarendon, Oxford, 1995).
- ²⁴D. G. Pettifor, in *Solid State Physics*, edited by H. Ehrenreich and D. Turnbull (Academic, New York, 1987), Vol. 40, p. 43.
- ²⁵A. P. Sutton, M. W. Finnis, D. G. Pettifor, and Y. Ohta, *J. Phys. C* **21**, 35 (1988).
- ²⁶A. J. Skinner and D. G. Pettifor, *J. Phys.: Condens. Matter* **3**, 2029 (1991).
- ²⁷J. Callaway, *Quantum Theory of the Solid State* (Academic, New York, 1974), Vol. 1, p. 297.
- ²⁸A. T. Paxton, *J. Phys. D* **29**, 1689 (1996).
- ²⁹C. Priester, G. Allan, and N. Lannoo, *Phys. Rev. B* **33**, 7164 (1986).
- ³⁰J. C. Cressoni and D. G. Pettifor, *J. Phys.: Condens. Matter* **3**, 495 (1991).
- ³¹D. E. Eastman, F. Himpsel, and J. F. van der Veen, *J. Vac. Sci. Technol.* **20**, 609 (1982).
- ³²D. A. Muller, P. E. Batson, and J. Silcox, *Phys. Rev. B* (to be published 1 November 1998).
- ³³D. A. Muller, Ph.D. thesis, Cornell University, Ithaca NY, 1996.
- ³⁴F. Cyrot-Lackmann, *Adv. Phys.* **16**, 393 (1967).
- ³⁵M. Weinert and R. E. Watson, *Phys. Rev. B* **51**, 17 168 (1995).
- ³⁶J. N. Anderson *et al.*, *Phys. Rev. B* **50**, 17 525 (1994).
- ³⁷L. Pauling, *The Nature of The Chemical Bond* (Cornell University Press, Ithaca, NY, 1960).
- ³⁸D. McMullan, P. J. Fallon, Y. Ito, and A. J. McGibbon, in *Proceedings of the 10th European Congress on Electron Microscopy (EUREM'92)*, Grenada, Spain, 1992, edited by A. Rios, J. M. Arias, L. Megias-Megias, and A. Lopez-Galindo, p. 103.
- ³⁹R. E. Burge and D. L. Misell, *Philos. Mag.* **18**, 251 (1968).
- ⁴⁰R. F. Egerton, B. G. Williams, and T. G. Sparrow, *Proc. R. Soc. London, Ser. A* **398**, 395 (1985).
- ⁴¹R. Hultgren *et al.*, *Selected Values of the Thermodynamic Properties of Binary Alloys* (American Society for Metals, Metals Park, OH, 1973).